CFD workshop on supersonc transport design, Tokyo, March 1998 i

Numerical simulation of the internal flow through the Mach 2 air-intake designed for NAL's experimental airplane

Hitoshi Fujiwara & Kimio Sakata
National Aerospace Laboratory, JAPAN

1 Introduction

National Aerospace Laboratory JAPAN is now developing an experimental supersonic airplane with two jet propulsion systems. An air-intake for the jet propulsion systems was designed and numerical simulation of the internal flow of the intake is being performed. An air-intake has a role of decelerating inlet supersonic air and supplying compressed subsonic air to a jet engine. An air–intake must stably supply enough low–Mach number, enough homogeneous air and enough mass flow to the engine in any flight condition. These points are inevitable for the airplane to flight safely. Moreover, it is better that the length of the intake is short, the pressure recovery is high and the external drag is small. Two important tools for designing an intake are wind tunnel test and numerical simulation. The result of numerical simulation is useful both for better designing and for performing wind tunnel test effectively and efficiently. In this paper, the designed intake is explained briefly and some of the results of the numerical simulation are shown.

2 Design

Figure 1 shows the side view of the designed intake. The design Mach number of the airplane is 2.0. At this inlet Mach number, a two dimensional external compression intake with three–shock system(two oblique and one normal) is the best choice in view of simplicity, operation stability and total pressure recovery. A 7° and 8° double-angled wedge was used to form the two oblique shock waves. The total pressure loss due to the three shock waves is less than 8 percent. At the throat the ramp and cowl internal surfaces are parallel. A short and compact square–to–round transition diffuser was used for subsonic compression. The length of the subsonic diffuser is four times as long as the throat hight. The large adverse pressure gradient of the internal flow may cause boundary layer separation. A bleed is located at the throat in order to prevent the separation and to stabilize the normal shock position. The cut–back side walls are applied in order to suppress the interaction between the side wall boundary layer and the oblique shocks. Figure 2 shows the schematic view of the intake.

3 Numerical Methods

Three dimensional Reynolds averaged, Navier–Stokes equations were solved with a low Reynolds number k–ϵ turbulence model. A TVD high resolution scheme was used to evaluate the spatial difference. For time advancement, an implicit method was adopted. Figure 3 shows the computational domains used in the simulation. The red domain is added to prevent the shock wave reflection at the boundary of the

internal flow domain. Downstream of the intake, a throat is added to control the volume flow quantity through the duct. The normal shock position is determined by the volume flow quantity. Table 1 shows the three cases simulated in this study. The effect of the throat bleed and that of side walls cut-back are examined by comparing the results of the three cases. The wall boundary conditions of the simulation S2 is shown in Figure 4. The slip wall boundary condition is used on the red region, where the boundary layer is completely removed. However, the sideway spillage cannot be taken into account in this simulation. The grid points distribution in the cross section is shown in figure 5. The numbers of the grid points are 61 for the radial, 85 for the circumferential and 80 for the streamwise directions.

	throat bleed	sidewall cutback
S1	NO	NO
S2	YES	NO
S3	NO	YES

4 Results: the effect of side walls

Figure 6 shows the Mach number distribution on the central symmetric surface of the simulation S1 without bleed and without cut-back of side walls. Oblique and normal shock waves are well simulated. The boundary layer on the lower wall separates just behind the normal shock causing a large recirculation. This phenomenon can be also observed in the total pressure recovery distribution on the cross sections shown in figure 7. The large total pressure loss in the lower half part in the sections is due to the separation. On the other hand, a loss in the upper right part is due to the interaction between the oblique shock waves and the side walls. Figure 8 shows the total pressure recovery distribution of the simulation S2 with the cut-back side walls. The pressure loss in the upper right part is removed in this simulation, showing that the cut-back side walls is useful for suppression of the interaction between the oblique shock waves and the side walls. A large cut-back means the large sideway spillage. Therefore, the suppression of the interaction should be pursued with minimum cut-back on the side walls. This is one of the future studies.

The accuracy of the numerical simulation is largely dependent on the turbulence model included. The eddy viscosity distribution obtained by using a low-Re k-ϵ turbulence model is shown in figure 9. As the eddy viscosity is usually large only in turbulent boundary layer, it can be said that the k-ϵ model gives a correct distribution. Figure 10 shows the distribution obtained by using Baldwin and Lomax algebraic turbulence model. B-L model, on the contrary, shows a poor prediction because the shock waves have a bad effect on the F-function used in the model. This implies that B-L model should be carfully used in the simulation of internal flow. In this following analysis, only the k-ϵ model is used.

5 Results: the effect of the throat bleed

The throat bleed was taken into account in the simulation S3. A cavity is added just below the ramp surface at the throat. There is a slit at the throat, thorough which some of the internal flow is sucked into the cavity. The cavity is bounded by slip walls, except the bottom surface which is opened to the external flow(cf. figure 11).

Figure 12 shows the Mach number distribution of the simulation with the bleed at supercritical operation. An expansion wave appears because the streamlines of the internal flow near the cavity bend toward the wall. The expansion wave reaches to the normal shock causing the increase of the local upstream Mach number and decrease of the local downstream Mach number of the normal shock. In this way, a momentum defect region comes out downstream of the interaction point.

Figure 13 shows the Mach number distribution at critical operation. There is also the expansion wave and the momentum defect region. The separation point is delayed a lot although the effect of the momentum defect region is so large that there is still a recirculation. The close view near the slip is shown in figure 14. The streamline of the internal flow near the wall bends toward the wall, while the core flow, which is not affected by the suction, is going straight. The large momentum defect region exists between the two differently directed flows.

When the volume flux quantity is decreased more, a part of the normal shock comes out of the duct, although the foot of the shock is still on the lip of the slit(cf. figure 15). The velocity defect region is not observed in this case. At this subcritical operation, the separation is much delayed. This phenomenon can be explained as follows: figure 16 shows the close view near the slit. At the subcritical operation, not only the flow near the wall but also the core flow is going toward the lower wall, therefore, a lot of momentum is supplied to the wall layer which prevents the boundary layer separation.

6 summary and future studies

Numerical simulation of the internal flow through the intake for the NAL's experimental airplane was performed. The effect of side walls and the throat bleed were examined. The followings are future studies:

1. To examine numerically the effect of the bleed flow quantity on the flow field.
2. To compare the numerical simulation with the results of the wind tunnel test.

To suppress the flow separation, the following items are being considered:

1. Reduction of the turning angle at the supersonic stage.
2. Reverse angle on the ramp surface at the throat.
3. Vortex Generator or blowing on the diffuser surface.

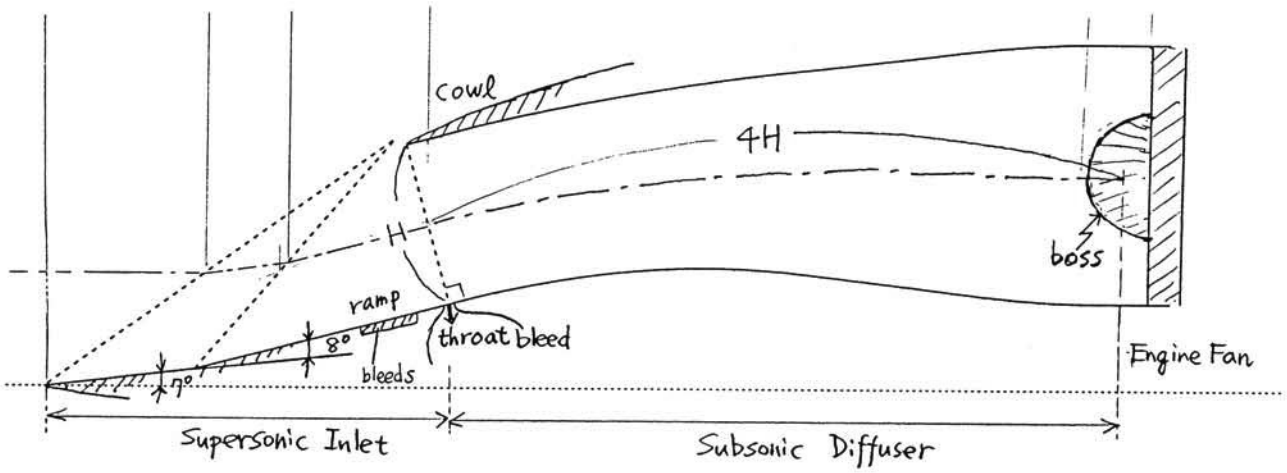

Figure 1: The air-intake for NAL SST(side view)

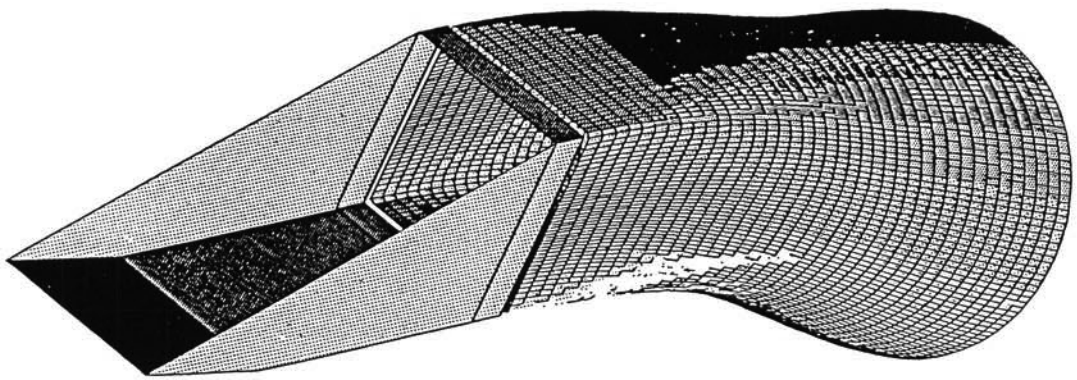

Figure 2: The schematic view of the air-intake

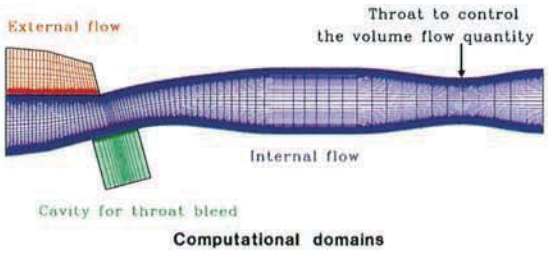

Figure 3: computational domains

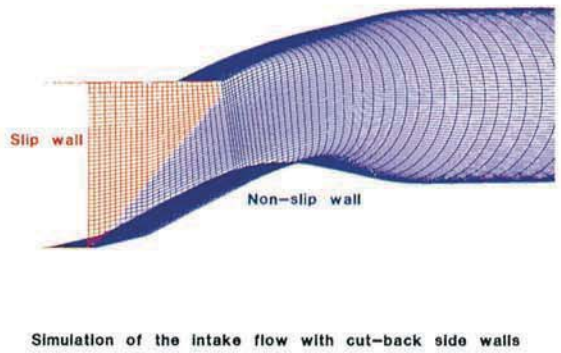

Figure 4: boundary conditions for cut-back side walls

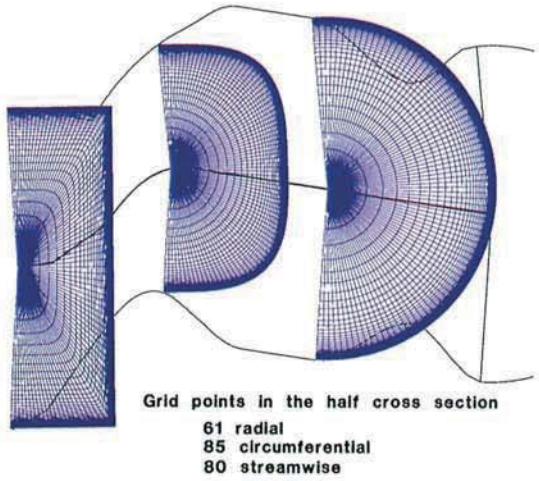

Figure 5: grid points distribution on the cross sections

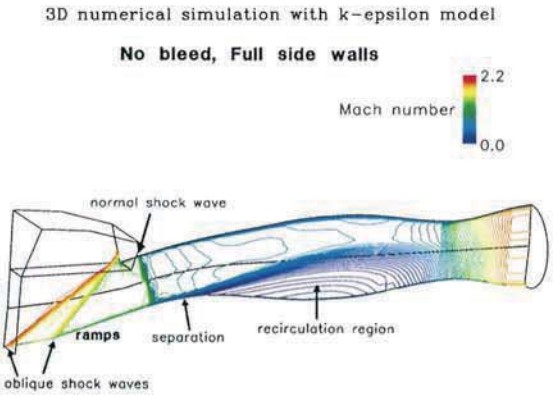

Figure 6: Mach number distribution

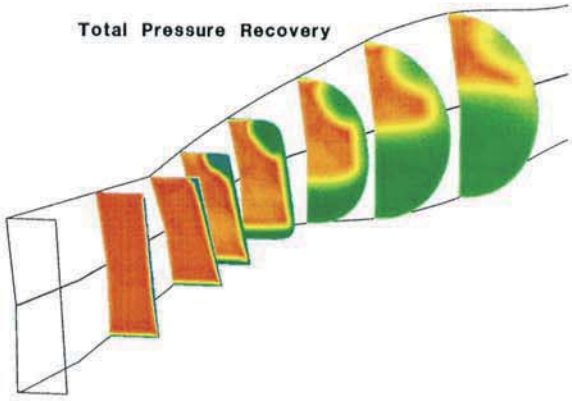

Figure 7: total pressure recovery(with full side walls)

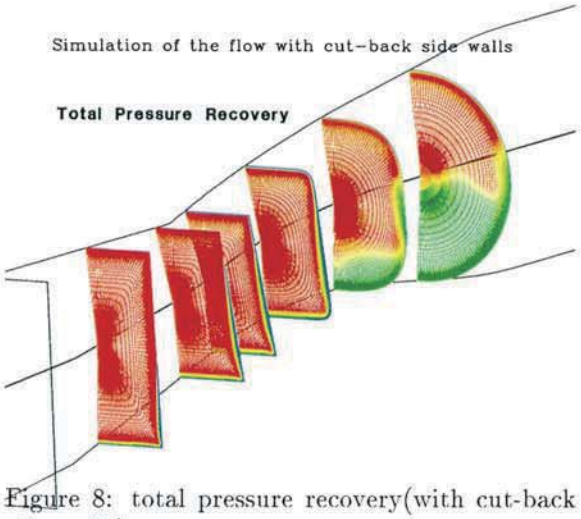

Figure 8: total pressure recovery(with cut-back side walls)

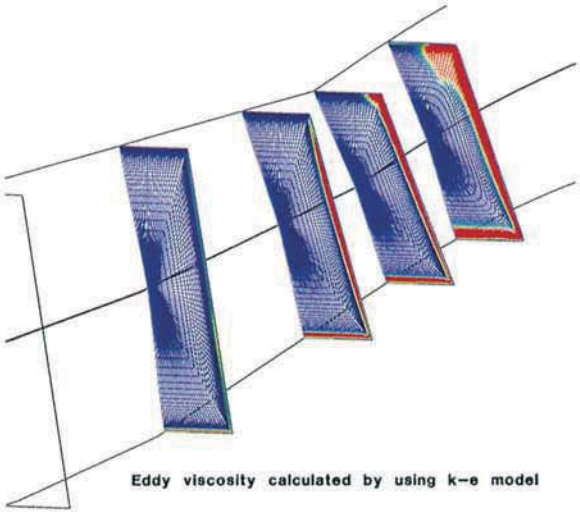

Figure 9: eddy viscosity distribution by k ϵ model

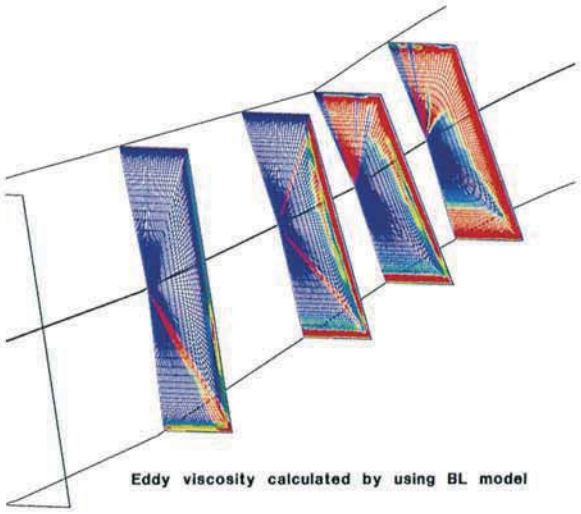

Figure 10: eddy viscosity distribution by BL model

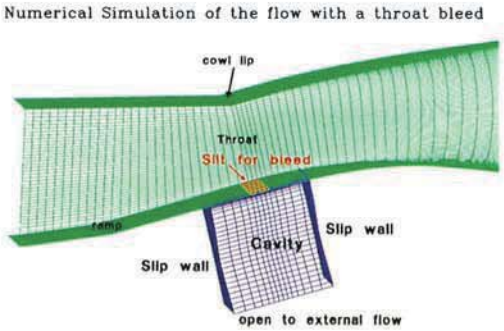

Figure 11: computational domains for the simulation with a bleed

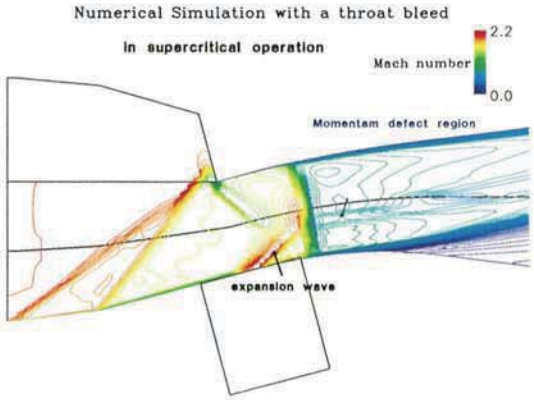

Figure 12: Mach number distribution at supercritical operation

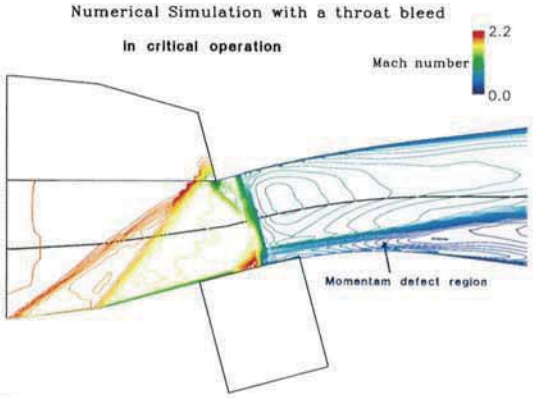

Figure 13: Mach number distribution at critical operation

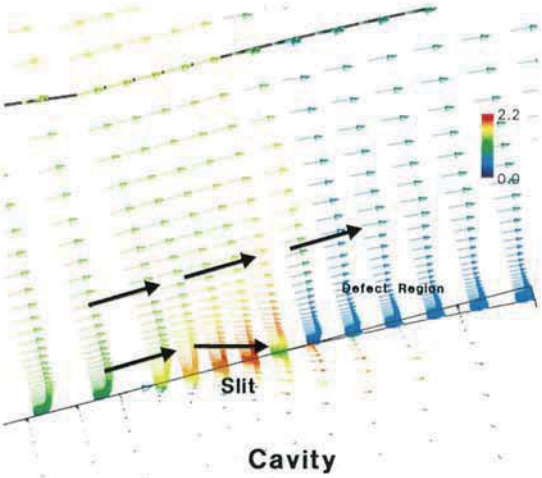

Figure 14: Close view near the slit at critical operation

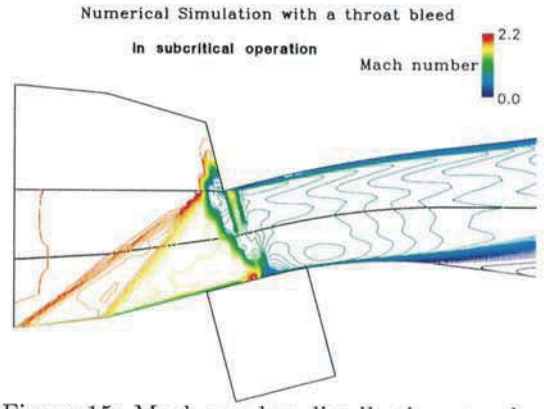

Figure 15: Mach number distribution at subcritical operation

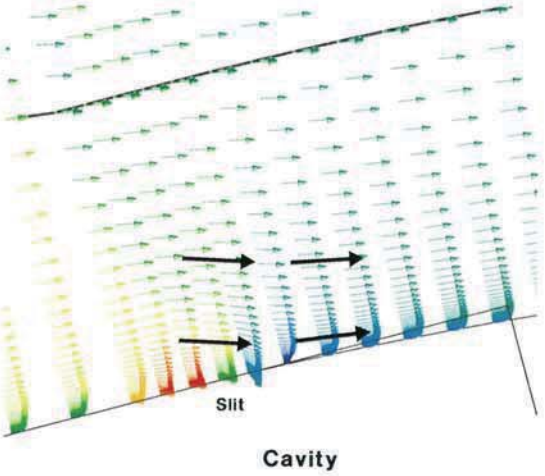

Figure 16: Close view near the slit at subcritical operation